

## Supplementary Material

### Numerical Model Development

To simulate lateral channel incision via meandering, we employ Howard and Knutson's (1984) kinematic model for river meandering. Although more mechanistically explicit approaches exist for computing velocity perturbations and hence erosion induced by meandering flow (Johannesson and Parker, 1989), here we employ Howard and Knutson (1984) because it is numerically efficient and represents the simplest physically justifiable approach that generates realistic meandering behavior without requiring specific erosion mechanisms, which remain uncertain.

Formally, the rate of channel migration in the model is given by solving the following convolution integral at every node in the river domain:

$$R_l(s) = k[\Omega R_o(s) + [\Gamma \int_0^\infty R_o(s - \xi) G(\xi) d\xi] [\int_0^\infty G(\xi) d\xi]^{-1}] \quad (1)$$

In Equation 1,  $R_l$  and  $R_o$  are the adjusted and the nominal channel migrations rates, respectively (Howard and Knutson, 1984). Nominal migration rates are calculated from the dimensionless curvature given by the ratio of the local radius of curvature,  $R$ , to the channel width,  $W$ .  $R_o(s - \xi)$  in Equation 1 is the nominal migration rate at a distance  $\xi$  upstream from  $s$ , where  $s$  is measured downstream from the river headwaters.  $\Omega$  and  $\Gamma$  are weighting parameters (Howard and Knutson, 1984).  $G(\xi)$  is an upstream weighting function given by:

$$G(\xi) = e^{-\chi \xi}, \quad (2)$$

where

$$\chi = k 2 C_f / h, \quad (3)$$

and  $k$  is unity,  $C_f$  is the dimensionless Chézy friction factor, and  $h$  is the channel depth (Howard and Knutson, 1984).

Meander wavelength in the Howard and Knutson (1984) model is determined by Equation 3, a result also verified with a more complete flow model (Edwards and Smith, 2002). Because for a given channel slope the height of a knickpoint generated from a cutoff meander is proportional to the meander wavelength, we adjusted the parameters in Equation 3 so that meanders with a wavelength comparable to those on the Smith River were generated in the numerical model.

In the simulation shown in the paper, we prescribed nominal migration rates such that when integrated in Equation 1, they yielded a relationship between curvature and migration rate that is consistent with what is typically observed in meandering channels (Hooke, 2007), albeit with rates that are comparable to bedrock rather than alluvial channel migration rates (Fig. DR1). We use the following relationships for nominal migration rates:

$$R/W \leq C^*,$$

$$R_o = k_l (R/W) \quad (4a)$$

$$W/R > C^*,$$

$$R_o = k_l C^{*2} (R/W)^{-1} \quad (4b)$$

In equation 4a and 4b,  $C^*$  is a critical non-dimensional curvature value, and  $k_l$  is a lateral erosion rate constant.

Vertical incision in the model,  $v(s)$ , is assumed to be linearly proportional to mean channel shear stress ( $\tau$ ),

$$v(s) = k_v \tau = k_v \rho_w g h S, \quad (5)$$

where  $\rho_w$  is the density of water,  $g$  is the acceleration due to gravity,  $h$  is channel depth,  $S$  is channel slope, and  $k_v$  is a vertical incision rate constant that we tuned to yield steady state channel gradients that are comparable to the Smith River,  $\sim 0.003$ . Again, although there are more mechanistically explicit approaches to computing vertical incision (Sklar and Dietrich, 2004), we choose the simplest physically defensible approach that permits coupling between lateral and vertical incision. The essential assumption of the vertical incision model is that river incision is fundamentally limited by the deposition of alluvial cover rather than the availability of erosive tools (Sklar and Dietrich, 2004). This results in a positive relationship between shear stress and incision rate when the channel is above the threshold for particle motion (Sklar and Dietrich, 2004).

A ratio of lateral to vertical incision rate must be implicitly imposed in the numerical model, as the equations for both lateral and vertical incision require rate constants. In the Central Oregon Coast Ranges, rates of vertical river incision can be relatively well constrained to 0.1-0.3 mm/yr (Personius, 1995), and compare well with basin-averaged erosion rates based on sediment yields (0.05-0.08 mm/yr) (Reneau and Dietrich, 1991), and cosmogenic isotope based basin averaged-erosion rates ( $\sim 0.12$  mm/yr) (Heimsath et al., 2001). Lateral incision rates, with one exception (Almond et al., 2007), have never been constrained in the Central Oregon Coast Ranges.

To constrain lateral channel erosion rates, we extracted elevation profiles along the inside of bedrock river meander bends on the Smith River, in regions where river terraces were clearly visible (Fig. DR2). Assuming that the elevation profile along the ridge that follows the inside of a meander bend describes roughly both the vertical and lateral trajectory of the river (Almond et al., 2007), we take the average slope on the ridge line along the inside of a meander bend as an indication of a river's ratio of lateral to vertical incision during bend growth. Fig. DR2 shows elevation profiles from 14 meander bends on the Smith River extracted from LiDAR data. The data together suggest that the ratio of lateral to vertical incision on the Smith is  $\sim 7.3$ . We therefore choose a rate constant for vertical incision such that vertical incision rates are on average 0.1 mm/yr, in keeping with the various erosion rate estimates reported above. The lateral incision constant is set to yield long term bedrock meander bend migration rates that are approximately 7-8 times the average vertical incision rate, in keeping with Fig. DR2.

For the chosen parameters, model channels generally evolved to have sinuosity of between two and three, which brackets the sinuosity of the Smith River, 2.7 (Fig. DR3).

In alluvial rivers, the rate of bend migration should depend on channel slope in most settings because slope scales the local boundary shear stress (e.g., Dietrich, 1987), and it is for this reason that Howard and Knutson (1984) incorporate a lateral erosion rule with a (mean) slope dependence. However, in our modeling, coupling Howard and Knutson (1984), as originally conceived, with a slope dependent vertical incision rule would result in a simulation where strath terraces would not form. This is because pulses of vertical incision would be accompanied by pulses of lateral planation, resulting in linear rather than stepped topographic profiles on the insides of river bends. Additionally, our field observations and analysis of LiDAR data from the Smith River indicate that upstream propagating incision waves do not result in enhanced lateral planation on actively growing bedrock meander bends, as would be expected if the rate of bend migration was accelerated by passing knickpoints. On the contrary, Fig. DR4 shows that the passage of the upstream migrating incision wave generated from the cutoff in Fig. 3 triggered a change from dominantly lateral to dominantly vertical incision. This is indicated by the downhill increase in the topographic slope on the inside of the bend, which records the pulse of vertical incision from the passing knickpoint.

We speculate that because propagating knickpoints commonly form horseshoe-shaped waterfalls or cut slots that are narrower than the channel upstream (e.g., Fig. DR4), they can disrupt the pattern of fluid flow that otherwise gives rise to high fluid stresses on the outside of river bends. In particular, a horseshoe-shaped waterfall that spans the channel (e.g., Pasternack et al., 2006) or a narrow slot or inner channel formed by a propagating knickpoint (e.g., Yanites et al., 2010) both result in flow convergence towards the center of a channel (Pasternack et al., 2006), even in a super-critical flow (Haviv et al., 2006). Because convergence could, in turn, result in acceleration of fluid away from the outside of the bend and towards the center of the channel, it could thereby reduce the stress on the outside of the bend. A further contributor would be that the knickpoint strips the alluvial cover, leading to a non-linear increase in local vertical incision rate as it depends on boundary shear stress (Sklar and Dietrich, 2004). Our model does not account for alluvial cover dynamics.

Thus, changes in local channel slope triggered by knickpoints in the model, which in turn change the local stress in the channel, do not result in changes in the rate of lateral channel migration in the model. Because the mean slope of the channel does not change appreciably during the simulations, changes in channel migration are therefore only driven by changes in planform curvature in the model. This choice in our modeling therefore represents an implicit assumption that meandering is disrupted where slope perturbations occur along the channel.

Additionally, because our own field observations in regions of bedrock meandering suggest that channel banks weather to suspended or wash load (and during bank failures shed gravel material that quickly falls apart due to wetting and drying), there is no feedback between the height of the escarpment on the outside of a bend and the rate of migration, as might otherwise be expected in a setting where bed load is added to the channel during lateral motion.

Although Equation 1 is intended to be integrated upstream infinitely, in the simulation the integration is carried out only to 30 nodes upstream of the node of interest. For the node spacing and parameters used in the simulation (Table DR1), the value of Equation 2 for the chosen parameters is negligible at well

shorter than 30 nodes upstream, thereby justifying this slight approximation to Equation 1. However, as a consequence of this numerical scheme, the 30 nodes at the upstream end of the domain are fixed in the simulation and cannot migrate. Additionally, we fixed the 30 nodes at the downstream end of the boundary.

In the model, we keep the number of nodes constant, so the spacing between nodes during simulations varied. The downstream node has a fixed elevation boundary condition, and the rest of the profile is uplifted at the tectonic uplift rate, resulting in relative base-level fall in the model channel. The model is initiated with a planform and long profile generated from running the coupled model for the equivalent of 2,500,000 years on an initially low sinuosity channel planform with a uniformly sloping long profile. Width,  $\chi$  (which depends on depth and friction), and tectonic uplift rate are all held constant throughout the simulation.

Meander cutoffs occur in the model when the spacing (measured from the channel centerline) across the neck is less than half the node spacing along the channel.

### **Strath Terrace Identification**

Because there are no hill slope processes in the model, changes in hill slope gradient in the model result only from variation in the ratio of lateral to vertical erosion in the model. Hence transitions from terrace treads to risers, which we map in Fig. 1, are identified in the LiDAR data and in the numerical model output by abrupt downhill increases in hill slope gradients along the insides of meander bends (e.g., Figs. 2A and 2B).

**Table DR1.** Values of parameters used in the simulation.

Model Parameter	Value
$\Omega$	-1
$\Gamma$	2.5
$k_v (\text{Pa}^1 \text{m}^1 \text{s}^{-1})$	3.17E-12
$k_l (\text{m}^1 \text{s}^{-1})$	6.34E-12
Average Node Spacing (m)	113
dt (s)	3.15E+10
time of simulation (yr)	1.50E+06
$\chi (\text{m}^{-1})$	0.006
$C^*$	5
Uplift Rate ( $\text{m}^1 \text{yr}^1$ )	1.00E-04

**Movie DR1.** The movie depicts the evolution of the model channel. The upper panel shows a shaded relief image of the evolving topography during the simulation. The blue line indicates the location of the channel centerline. The lower pane shows the evolution of the channel elevation long profile during the simulation. The length of the river channel changes during the simulation due to meander growth and

cutoff. Therefore the river length is non-dimensionalized by the total length of channel. Channel width is 40 m in the simulation

## **References**

- Almond, P., Roering, J., and Hales, T.C., 2007, Using soil residence time to delineate spatial and temporal patterns of transient landscape response: *J. Geophys. Res.*, v. 112, p. F03S17.
- Dietrich, W.E., 1987, Mechanics of Flow and Sediment Transport in River Bends, *in* Richards, K.S., ed., *River Channels: Environment and Process*: Institute of British Geographers Special Publication Basil Blackwell, Inc, p. 179-227.
- Edwards, B.F., and Smith, D.H., 2002, River meandering dynamics: *Physical Review E*, v. 65, p. 046303.
- Haviv, I., Enzel, Y., Whipple, K.X., Zilberman, E., Stone, J., Matmon, A., and Fifield, L.K., 2006, Amplified erosion above waterfalls and oversteepened bedrock reaches: *J. Geophys. Res.*, v. 111, p. F04004.
- Heimsath, A.M., Dietrich, W.E., Nishiizumi, K., and Finkel, R.C., 2001, Stochastic processes of soil production and transport: erosion rates, topographic variation and cosmogenic nuclides in the Oregon Coast Range: *Earth Surface Processes and Landforms*, v. 26, p. 531-552.
- Hooke, J.M., 2007, Complexity, self-organisation and variation in behaviour in meandering rivers: *Geomorphology*, v. 91, p. 236-258.
- Howard, A.D., and Knutson, T.R., 1984, Sufficient conditions for river meandering: A simulation approach: *Water Resources Research*, v. 20, p. 1659–1667
- Johannesson, H., and Parker, G., 1989, Linear theory of river meanders, *in* Ikeda, S., and Parker, G., eds., *River Meandering*, American Geophysical Union, p. 181-204.
- Pasternack, G.B., Ellis, C.R., Leier, K.A., Vallé, B.L., and Marr, J.D., 2006, Convergent hydraulics at horseshoe steps in bedrock rivers: *Geomorphology*, v. 82, p. 126-145.
- Personius, S.F., 1995, Late Quaternary stream incision and uplift in the forearc of the Cascadia subduction zone, western Oregon: *Journal of Geophysical Research*, v. 100, p. 20,193–20,210.
- Reneau, S.L., and Dietrich, W.E., 1991, Erosion rates in the southern oregon coast range: Evidence for an equilibrium between hillslope erosion and sediment yield: *Earth Surface Processes and Landforms*, v. 16, p. 307-322.
- Sklar, L.S., and Dietrich, W.E., 2004, A mechanistic model for river incision into bedrock by saltating bed load: *Water Resources Research*, v. 40, p. W06301

Yanites, B.J., Tucker, G.E., Mueller, K.J., and Chen, Y.-G., 2010, How rivers react to large earthquakes: Evidence from central Taiwan: *Geology*, v. 38, p. 639-642.

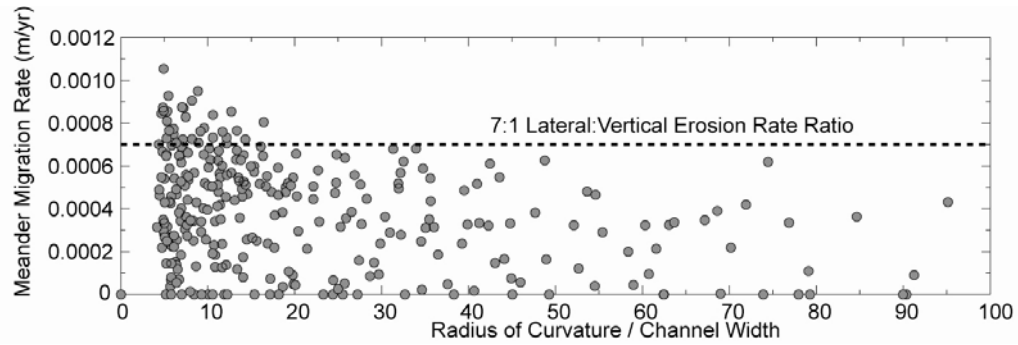


**Figure DR1.** Bend migration rate versus non-dimensional channel curvature for a numerical model iteration. The dashed line indicates the mean lateral erosion rate for bends on the Smith River.

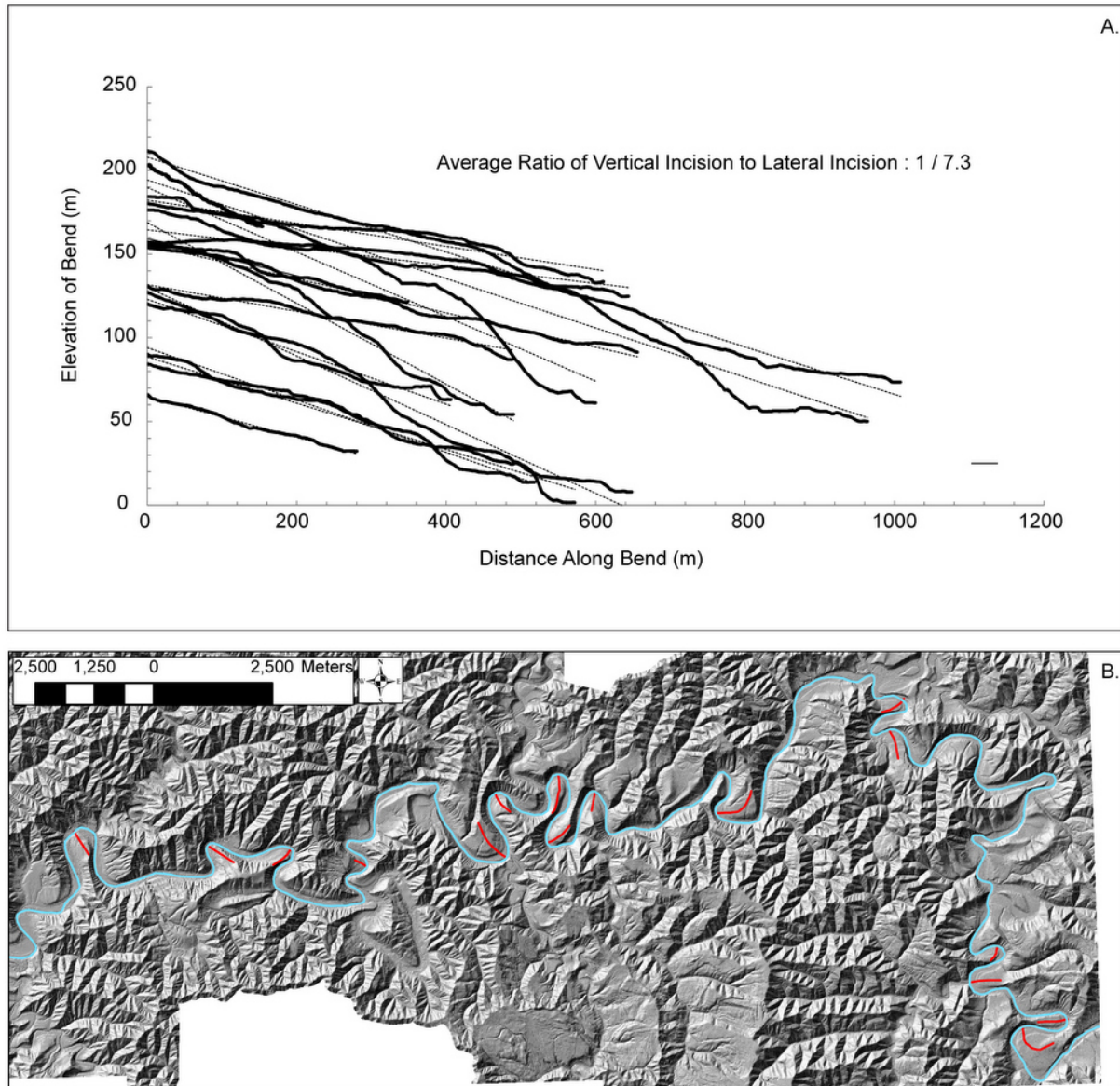


**Figure DR2.** A: Elevation profiles (solid black lines) and linear fits to elevation profiles (dotted lines) along ridge lines from the inside of active bedrock meanders with strath terraces along the Smith River. The average gradient of the 14 elevation profiles, which we take to be a proxy for the vertical:lateral erosion rate ratio, is 1/7.3. B: Locations of topographic profiles (red) shown in A.

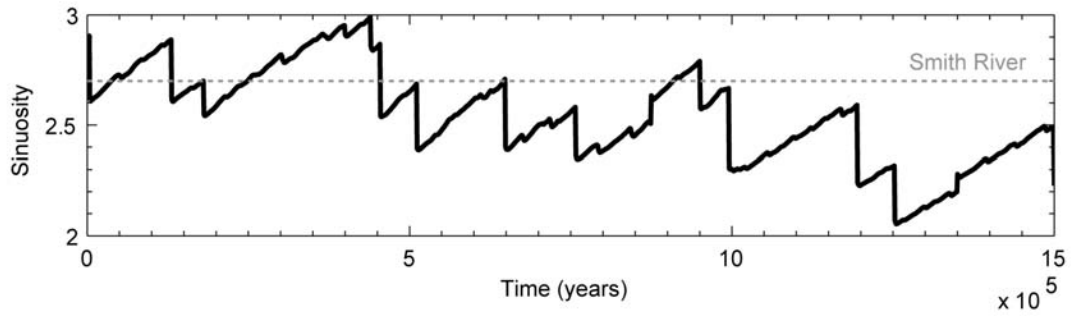


**Figure DR3.** Channel sinuosity (solid line) during the simulation shown in the paper. The dashed gray line indicates the average sinuosity of the Smith River over the reach shown in Figure 1A.



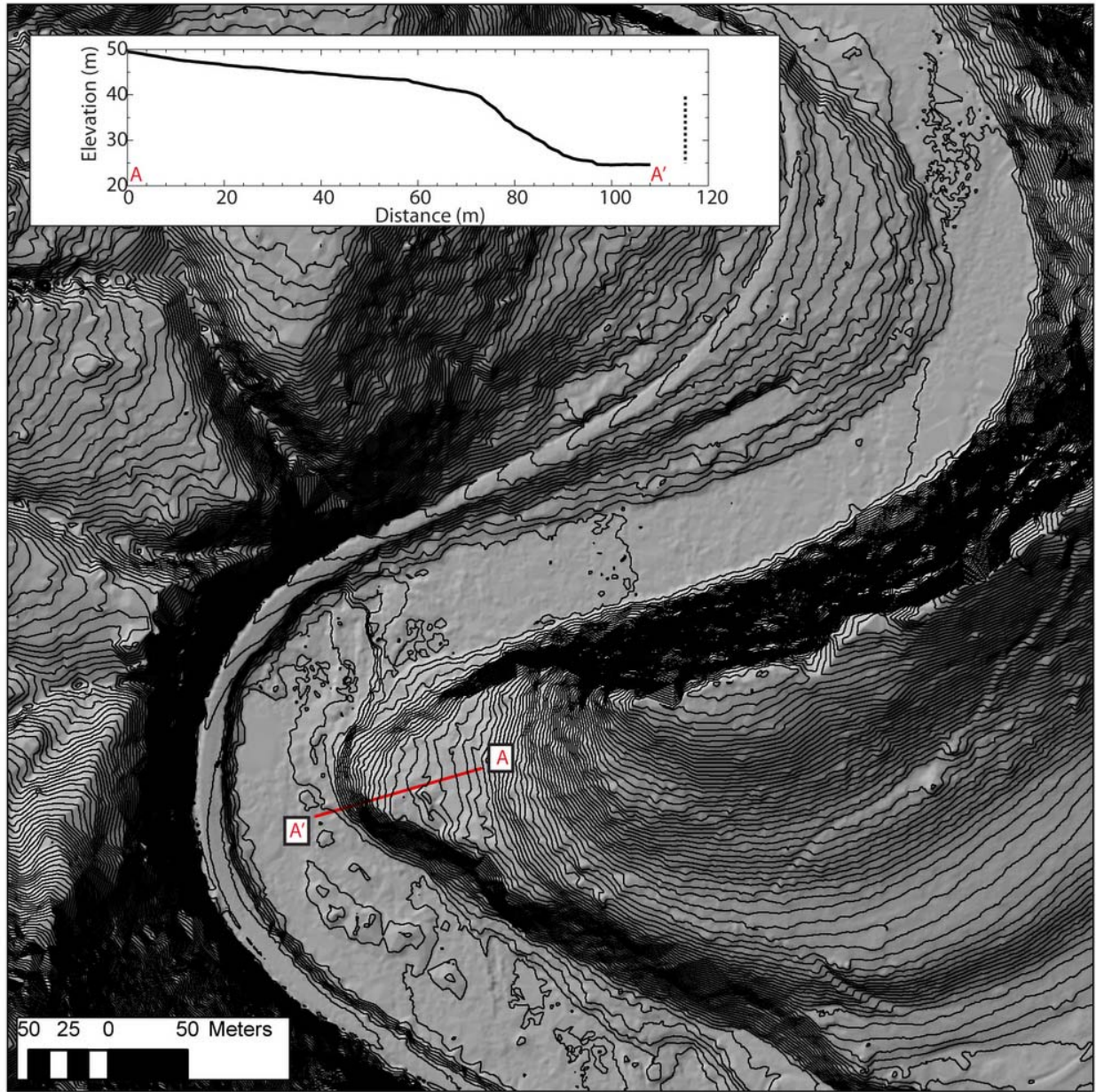


**Figure DR4.** 1-m interval LiDAR-derived contour map of Smith River Falls. The inset shows the elevation profile between A and A', and indicates that the passage of the meander cutoff-triggered knickpoint (just upstream of the cross-section line, also shown in Figure 3) has increased the ratio of vertical:lateral incision. The dashed vertical line in the inset indicates the approximate elevation drop around the abandoned bend. River flow is from the top of the page.